A MODEL STUDY ON THE ABSORBED DOSE OF RADIATION FOLLOWING RESPIRATORY INTAKE OF 238U3O8 AEROSOLS

A MODEL STUDY ON THE ABSORBED DOSE OF RADIATION FOLLOWING RESPIRATORY INTAKE OF $^{238}U_3O_8$ AEROSOLS

Carlo Canepa

Dipartimento di Chimica, Università di Torino, Via Pietro Giuria 7, 10125 Torino, Italy
Corresponding author. Tel.: +390116707530.
E-mail address: carlo.canepa@unito.it

ABSTRACT

Aerosols of depleted uranium oxides, formed upon high-energy impact of shells on hard targets during military operations, are able to disperse, reach the alveolar region of the lungs and be absorbed and distributed throughout various parts of the body. The absorbed particles are subjected to clearance in the upper respiratory tract, distribution to other body districts, dissolution, and excretion. While the soluble forms of uranium are known to deliver a small dose of radiation to the body due to their homogeneous distribution and the low specific activity of ^{238}U, ceramic particles exhibit a low dissolution rate and irradiate a limited volume of tissue for a long time with α particles with energy 4.267 MeV. The extent of the irradiated tissues depends on the radius of the particles and the total intake of uranium oxides. For the measured intake of U_3O_8 of a war veteran (15.51 μg) the number of particles ranges from 5.56×10^4 to 6.95×10^6 for sizes of $0.4 - 2.0$ μm. Modeling the distribution of the particles between two compartments of the body, the averaged dose absorbed in 20 years by tissues surrounding the particles and within the range of the α particles varies from 6.8 mGy to 0.85 Gy for lungs and 8.1 mGy to 1.0 Gy for the lymph nodes, respectively. Correspondingly, due to the clearance and redistribution, the mass irradiated by 2.0 μm particles falls in 20 years from 6.06 mg to 0.94 μg in the lungs and grows from zero to 1.0 mg in the lymph nodes. The estimated rate of formation of hydroxyl radicals upon radiolysis of water in the lungs and lymph nodes is 5.17×10^4 d^{-1} per cell after one year.

Keywords: depleted uranium; particles distribution; absorbed dose

INTRODUCTION

Depleted uranium (DU) is characterized by a reduced content of the isotope ^{235}U with respect to natural uranium and is obtained as a by-product of the enrichment process of natural and reprocessed uranium. It is used in military combat in various projectiles because it is readily available, pyrophoric, and it has a unique armor-piercing capability due to its high density. Upon high-energy impact, the shells of DU heat up, fragment and oxidize into a mixture of uranium oxides with various oxidation states[1], usually dominated by U_3O_8. The dispersed ceramic particles of DU oxides with sizes of the order of 1 μm are able to reach the alveolar region of the lungs upon inhalation. Whether the biological effects following the exposure to aerosols of DU oxides are responsible for the complex syndrome affecting the military and civilian populations around combat areas is still a matter of controversy[2,3,4,5]. The long half-life of the isotope ^{238}U ($\tau_{1/2} = 4.468 \times 10^9$ yr) makes its specific activity relatively low, and it is easy to show that the dose absorbed by the people exposed to DU aerosols is a small fraction of the background radiation. However, it is difficult to reconcile the low estimate of the radiation dose delivered to the whole body by the intake of depleted uranium[6,7,8,9] and the reports of the complex array of symptoms affecting war veterans and civilian populations, however anecdotal.

As a contribution to this issue, this work points out the small portion of an idealized body affected by the radiation delivered by a mass m_0 of U_3O_8 (molecular mass $\mu = 0.8421$ kg mol^{-1}, density $\rho_{U_3O_8} = 8326$ kg m^{-3}) in the form of particles of initial radius r_0, containing exclusively the isotope ^{238}U. It will be shown that depleted uranium particles are able to deliver a much higher radiation dose with respect to the soluble forms of uranium, albeit to a small mass of tissue.

The actual distribution of ^{238}U following an instantaneous respiratory intake of ceramic particles of U_3O_8 was modeled by Valdés[10], who described how the species containing ^{238}U distribute among lungs, lymph nodes, kidneys, bones, blood, and other tissues and are eventually excreted via the urine. The model developed in this work computes the amount of radiation absorbed by the tissue surrounding the particles in the two compartments of the body where the ceramic oxide particles mostly reside, i.e. the lungs and the lymph nodes. To partition the cumulative dose affecting all the different body compartments, one would have to solve a complete set of differential equations representing all fluxes among the compartments.

The calculation of the absorbed dose does not include the contribution from the beta decay of daughter radionuclides ^{234}Th ($\tau_{1/2} = 24.10$ d, $\lambda = 3.3288 \times 10^{-7}$ s^{-1}, β^- 0.0592 MeV) and ^{234m}Pa ($\tau_{1/2} = 1.159$ min, $\lambda = 9.9676 \times 10^{-3}$ s^{-1}, β^- 0.82 MeV), in secular equilibrium with ^{238}U ($\lambda = 4.9160 \times 10^{-18}$ s^{-1}, α 4.267 MeV) through the first three steps of the decay chain of ^{238}U

$$^{238}\mathrm{U} \xrightarrow{\alpha} {}^{234}\mathrm{Th} \xrightarrow{\beta^-} {}^{234\mathrm{m}}\mathrm{Pa} \xrightarrow{\beta^-} {}^{234}\mathrm{U}.$$

The contribution of the gamma emissions, the possible presence of ^{236}U, heavier actinides, and the residual ^{235}U in the particles are also neglected.

RESULTS AND DISCUSSION

We begin by taking into consideration the 13.153 μg intake of ^{238}U of a Persian Gulf War I veteran estimated by Valdés[10] from the analysis of a urine sample. This value is bracketed by the estimated 100 μg intake in the neighborhood of a burning tank hit by a 120 mm DU projectile and the corresponding intake of 0.8 μg at a distance of 200 m from the impact site[11]. At the breathing rate of 0.9 m^3 h^{-1} in a contaminated area with a DU air concentration of 1 μg m^{-3}, the assumed exposure of 13.153 μg would be reached in 17.23 h. The corresponding mass of U_3O_8 is $m_0 = 15.508$ μg. As we shall see, the mass of ^{238}U in the body is time-dependent because of the excretion

mechanisms acting after the exposure, and we indicate the instantaneous value of the mass with m. The number of ^{238}U nuclei at any given time is thus

$$N_U = 3\frac{m}{\mu}N_A, \quad (1)$$

(3 being the number of ^{238}U nuclei in each molecule of U_3O_8) and, at $t = 0$, we have $N_U = 3.3271 \times 10^{16}$, corresponding to the activity $\lambda N_U = 0.1636$ Bq. The average distance between n sources of α particles distributed in a body mass M_b is

$$d \cong \left(\frac{M_b}{\rho_w n}\right)^{1/3}. \quad (2)$$

If the uranium is in a soluble form, like a uranyl salt, we would have $n = N_U$, and the distribution in the body of both the ^{238}U and its α radiation may be considered homogeneous over the whole mass. In fact, for $M_b = 70$ kg, the average distance between ^{238}U nuclei would be 1.28 μm, smaller than the range R of the α particles themselves, 29.63 μm (ASTAR database)[12].
The power transferred to the body by the decay of ^{238}U is $P = \lambda N_U E_\alpha = 1.12 \times 10^{-13}$ W, where

$$E_\alpha = 4.267 \text{ MeV} \times 1.602 \times 10^{-13} \text{J MeV}^{-1} = 6.8325 \times 10^{-13} \text{ J} \quad (3)$$

is the energy per nuclear disintegration. The corresponding delivered dose rate ψ is P divided by the mass of the irradiated tissue, with units of a specific power, Gy d^{-1}. If the energy in Eq. (3) is multiplied by the corresponding weight factor for α particles (20), we obtain the effective dose rate in Sv d^{-1}. Neglecting the effect of the relatively short biological half-life of soluble forms of uranium in the human body (≈ 1 d), we obtain that the dose delivered to the body ($M_b = 70$ kg) by the homogeneous distribution is 1.01×10^{-6} Sv yr^{-1}, a small fraction of the average background radiation dose of $2 - 3 \times 10^{-3}$ Sv yr^{-1}. This approximate result corresponds to 6.16×10^{-6} Sv Bq^{-1} for one year, in agreement with the reported value of the effective absorbed dose following a hypothetical single acute inhalation of 90 Bq (6.0×10^{-6} Sv Bq^{-1})[7]. The corresponding dose conversion factor is 6.5×10^{-5} Sv mg^{-1} yr^{-1}, about one half of the accurate value 1.2×10^{-4} Sv mg^{-1} yr^{-1} [11].
On the other hand, if the particles are in the form of spheres of U_3O_8 with initial radius r_0, their number N_0 would be related to the mass by

$$m_0 = N_0 \rho_{U_3O_8} \frac{4}{3}\pi r_0^3. \quad (4)$$

The number of particles N_0 (listed in **Table 1**) for initial radius $0.4 \le r_0 \le 2.0$ μm is $5.56 \times 10^4 \le N_0 \le 6.95 \times 10^6$. In this case, $n = N_0$ and the average distance between the α sources according to Eq. (2) is $2.16 \times 10^3 \le d \le 1.08 \times 10^4$ μm, 2-3 orders of magnitude larger than the range of the α particles. Consequently, the distribution of ^{238}U in the body may not be considered homogeneous, each particle delivering its radiation only to a sphere of radius $R = 29.63$ μm and mass $M_\alpha = \rho_w(4/3)\pi R^3$. Since the range of the α particles emitted by ^{238}U in uranium (7.46 μm) exceeds the size of the particles, we do not correct for self-absorption. In this case the absorbed energy is not distributed to the whole body, but limited by the range of the α particles to the time-dependent mass

$$M = NM_\alpha, \quad (5)$$

where we have identified the body density with the density of water ρ_w. Typical values of M_0 are a fraction of a gram. The irradiated energy will be averaged over the limited portions of the organs directly affected by the α radiation. This approach leads to considerably higher doses with respect to the standard methods, which assess doses by averaging over the whole tissue mass. The initial dose rate delivered by N_0 particles thus is

$$\psi_0 = \lambda \frac{3m_0 N_A}{\mu} \frac{E_\alpha}{N_0 M_\alpha}, \quad (6)$$

independent of the number of the particles since the ratio m_0/N_0 depends only on r_0 and the density of the material, according to Eq. (4). The range of the initial dose rate for $0.4 \leq r_0 \leq 2.0$ μm is $9.32 \times 10^{-2} \leq \psi_0 \leq 11.6\ \mathrm{Sv\,yr^{-1}}$, to be compared to $1.01 \times 10^{-6}\ \mathrm{Sv\,yr^{-1}}$ for the homogeneous system. Since the dissolved fraction of U_3O_8 gives a negligible contribution to the radiation dose, we only keep track of the uranium still present in the body as undissolved particles. The particles are assumed to distribute in two compartments: the lungs, where the particles are subjected to both dissolution and clearance, and the interstitium and lymph nodes, identified by Valdés[10] as the main repository of undissolved particles, where the particles are only subjected to dissolution. The transport of the particles from the lungs into the lymph nodes exhibits the rate coefficient $\lambda_a = 2.0 \times 10^{-4}\ \mathrm{d^{-1}}$, while the clearance towards the mucociliary escalator takes place with the rate coefficient $\lambda_c = 1.0 \times 10^{-3}\ \mathrm{d^{-1}}$ [10], both processes being mediated by the alveolar macrophages.

Since the particles dissolve over time regardless of their location, their number is actually time-dependent. To compute the amount of undissolved U_3O_8 taking into account the dissolution rate of U_3O_8 particles, we follow the process as described by Chazel *et al.*, [7] that is the sum of a rapidly dissolving fraction f with rate coefficient λ_1 and a slowly dissolving fraction $1-f$ with rate coefficient λ_2. We thus have two sets of rate coefficients: the transport coefficients λ_a and λ_c, governing the transfer of particles, and the dissolution coefficients λ_1 and λ_2, that remove uranium from the particles. The relevant differential equations for transport and dissolution (two for the rapidly-dissolving fractions, x_1 and y_1, and two for the slowly-dissolving fractions, x_2 and y_2, where x and y represent the mass of U_3O_8 in lungs and lymph nodes, respectively) are

$$\dot{x}_i = -(\lambda_c + \lambda_a + \lambda_i)x_i, \quad (7)$$

with solution

$$m_x/m_0 = s(u_1 + u_2), \quad (8)$$

where

$$m_x = x_1 + x_2, \quad s = e^{-(\lambda_c+\lambda_a)t},$$

$$u_1 = f e^{-\lambda_1 t}, \quad u_2 = (1-f)e^{-\lambda_2 t}.$$

For the rapidly and slowly-dissolving fraction in the lymph nodes (y_i)

$$\dot{y}_i = \lambda_a x_i - \lambda_i y_i, \quad (9)$$

with solution

$$m_y/m_0 = \frac{\lambda_a}{\lambda_c + \lambda_a}(1-s)(u_1+u_2), \quad (10)$$

where $m_y = y_1 + y_2$. Plots of m_x/m_0 and m_y/m_0 versus time are shown in **Fig. 1**. The values of the rapidly dissolving fraction and of the dissolution coefficients are $f = 0.57$, $\lambda_1 = 0.07\ \mathrm{d}^{-1}$, and $\lambda_2 = 3.4 \times 10^{-4}\ \mathrm{d}^{-1}$, indicating a biological half-life of the slow-dissolving fraction of 5.58 yr. For comparison, the rate coefficient for the dissolution of U_3O_8 particles in alveolar macrophages given by Poncy *et al.* [13] is $3.9 \times 10^{-4}\ \mathrm{d}^{-1}$. Thus the total mass $m = m_x + m_y$ in the form of particles is

$$m/m_0 = \frac{s\lambda_c + \lambda_a}{\lambda_c + \lambda_a}(u_1+u_2), \quad (11)$$

exhibiting a mean life for the slowly-dissolving fraction approximately equal to $(\lambda_c + \lambda_a + \lambda_2)^{-1} = 1.78$ yr. Defining

$$v_1 = \frac{f - su_1}{\lambda_c + \lambda_a + \lambda_1}, \quad v_2 = \frac{1 - f - su_2}{\lambda_c + \lambda_a + \lambda_2},$$

the corresponding cleared and dissolved fractions of the initial intake are $\lambda_c(v_1+v_2)$ and $(\lambda_a/(\lambda_c+\lambda_a))(1-u_1-u_2+\lambda_1 v_1+\lambda_2 v_2)$, respectively. The excretion of the uranium content of the body after dissolution is almost exclusively urinary, and its distribution was modeled by Wrenn *et al.* [14]. According to the model presented here, the total normalized dissolution rate is $(\lambda_c+\lambda_a)^{-1}\big((s\lambda_c+\lambda_a)\lambda_1 u_1 + \lambda_a\lambda_2 u_2\big)$, starting at $4 \times 10^{-2}\ \mathrm{d}^{-1}$ at $t = 0$ and rapidly dropping to $4 \times 10^{-5}\ \mathrm{d}^{-1}$ after 110 days.

The irradiated mass was computed for each compartment according to Eq. (5) with the time-dependent number of particles given by

$$\dot{N}_x = -(\lambda_c + \lambda_a)N_x, \quad (12)$$

$$\dot{N}_y = \lambda_a N_x, \quad (13)$$

with solutions

$$N_x/N_0 = s, \quad (14)$$

$$N_y/N_0 = \frac{\lambda_a}{\lambda_c + \lambda_a}(1-s), \quad (15)$$

and

$$N/N_0 = \frac{s\lambda_c + \lambda_a}{\lambda_c + \lambda_a}. \quad (16)$$

The quantities N_x/N_0 and N_y/N_0 are shown in **Fig. 2**, and the corresponding masses M_x and M_y are obtained multiplying by the mass of tissue M_α irradiated by a single particle. The result reproduces Valdés' observation that a fraction ~10% of the initial intake is permanently sequestered in the lymph nodes. The values of M_x and M_y reported in **Tables 2** and **3** depend on N_0, and we can see that the amount of irradiated mass differ considerably in the two compartments.

The time-dependent dose rates delivered to the two compartments ($z = x, y$) according to Eqs. (8) and (10) are

$$\psi_z/\psi_0 = u_1 + u_2, \quad (17)$$

with the specific dose rate at $t = 0$ defined by Eq. (6). The dose rate delivered to the lungs and lymph nodes is the sum of two exponentials, decreasing in time from the initial value ψ_0, as shown in **Fig. 3**. The dose rate at $t = 0$ is reported in **Table 1** for specific values of the initial radius of the particles, along with the number of irradiated cells assuming a cell number density $\rho_c = 1.43 \times 10^{10}$ cell kg^{-1}. With this value of the cell number density, we obtain the constant ratio 1.56 cells/particle. The initial content m_0 of ^{238}U in the body and the size of the particles determine the extent of the irradiated mass M_z in each compartment, the radiation being delivered to only a small amount of tissue for a prolonged period of time. Both in the lungs and the lymph nodes the full 20 yr dose from particles of size 2 μm is absorbed by ~1 mg.

The total dose is independent of the number of particles (as is ψ_0) and of the transport coefficients, and is obtained by integration of the dose rate as

$$D_z = \int_0^t \psi_z(\xi) d\xi, \quad (18)$$

affording the expression

$$D_z/\psi_0 = \lambda_1^{-1}(f - u_1) + \lambda_2^{-1}(1 - f - u_2) \quad (19)$$

for each compartment. In the absence of both transport and dissolution we would have $D_z/\psi_0 = t$. The plot of Eq. (19) in **Fig. 4** shows that after 5 yr the dose reaches 0.12 Gy, reaching 0.25 Gy after 30 yr. An average quantity that takes into account the extent of the irradiated tissue in each compartment would be

$$< D_z >= \int_0^t \psi_z \frac{N_z}{N} d\xi, \quad (20)$$

in the assumption that the dissolved forms of ^{238}U are rapidly excreted and only the surviving particles contribute significantly to the total radiation dose. The averaged dose defined by Eq. (20) correctly depends on both the transport and dissolution rate coefficients, and the total dose D_z is partitioned in the two compartments, since $< D_x > + < D_y >= D_z$.

The averaged dose could also be defined with respect to the initial number of particles N_0, affording

$$< D_x >= \int_0^t \psi_x \frac{N_x}{N_0} d\xi = \psi_0(v_1 + v_2), \quad (21)$$

and

$$< D_y >= \int_0^t \psi_y \frac{N_y}{N_0} d\xi = \psi_0 \left[\lambda_a \left(\frac{v_1}{\lambda_1} + \frac{v_2}{\lambda_2}\right) - \frac{\lambda_a}{\lambda_c + \lambda_a}(1 - s)\left(\frac{u_1}{\lambda_1} + \frac{u_2}{\lambda_2}\right)\right]. \quad (22)$$

However, in this case the sum $< D_x > + < D_y >$ would not amount to D_z as defined by Eq. (19) and the definition making use of the weight N_z/N_0 would give an unrealistically small averaged dose in both compartments for a large clearance rate (large λ_c), since

$$\lim_{\lambda_c \to \infty} \frac{N_x}{N_0} = \lim_{\lambda_c \to \infty} e^{-(\lambda_c + \lambda_a)t} = 0,$$

$$\lim_{\lambda_c \to \infty} \frac{N_y}{N_0} = \lim_{\lambda_c \to \infty} \frac{\lambda_a}{\lambda_c + \lambda_a} \left(1 - e^{-(\lambda_c + \lambda_a)t}\right) = 0,$$

while

$$\lim_{\lambda_c \to \infty} \frac{N_x}{N} = \lim_{\lambda_c \to \infty} \frac{(\lambda_c + \lambda_a) e^{-(\lambda_c + \lambda_a)t}}{\lambda_c e^{-(\lambda_c + \lambda_a)t} + \lambda_a} = 0$$

and

$$\lim_{\lambda_c \to \infty} \frac{N_y}{N} = \lim_{\lambda_c \to \infty} \frac{\lambda_a \left(1 - e^{-(\lambda_c + \lambda_a)t}\right)}{\lambda_c e^{-(\lambda_c + \lambda_a)t} + \lambda_a} = 1$$

giving $\lim_{\lambda_c \to \infty} < D_y > = D_y$. For this reason we choose to compute the average doses with Eq. (20).

In this work, the dose rate ψ_z, the dose D_z, and the averaged dose $< D_z >$ are all computed for an irradiated mass fixed in space. Since the particles of U_3O_8 are being transported by the macrophages while they irradiate, the computed values are accurate only in the assumption that the actual time spent by the particles migrating inside the macrophages is negligible compared to the effective transport mean time λ_a^{-1}. Values of ψ_z, D_z, and $< D_z >$ are reported as functions of r_0 and t in **Tables 4** and **5-7** for the lungs and lymph node compartments. From the time-dependent plots of $< D_x >$ and $< D_y >$ shown in **Fig. 4**, we can see that the dose delivered to the lungs by 1 μm particles rises sharply and levels off after ∼10 yr at a maximum of ∼0.11 Gy, while the corresponding averaged specific dose delivered to the lymph nodes reaches 0.14 Gy and is still increasing even 30 yr after the exposure. The averaged doses delivered to the two compartments are comparable, with the dose to the first compartment, being the location of the initial intake, dominating for the first 15 yr. The absorbed dose (albeit by a small mass of tissue, as made clear by the data in **Tables 2-3**) may be divided by the total initial mass of $^{238}U_3O_8$ to obtain, 20 yr after the intake of 2 μm particles, the dose conversion factors 55.0 and 65.1 Gy mg^{-1} for the lungs and lymph nodes, respectively. For the homogeneous system the corresponding value reported by Bem and Bou-Rabee[11] is 1.2×10^{-4} Sv mg^{-1}. The wide separation between these two conversion factors summarizes the difference between the homogeneous and the non-homogeneous system. The 13.153 μg intake of DU might seem negligible compared both to the average content in the human body of 56 μg and the annual intake of 460 μg by ingestion of food and water[6], but if the radionuclide is concentrated in particles its radiation only targets a small mass of tissue for an extended period of time.

The α particles have also been shown to possess a specific action on DNA, and considerable chemical toxicity comes from the various chemical forms of uranium[15] as well. As a crude approximation to the chemical damage to which the irradiated masses M_x and M_y are subjected, we may estimate the rate of unspecific bond breaking per cell $\dot{B}_z$ in the two compartments multiplying ψ_z by the factor $N_A/(E_{bond}\rho_c)$ and assuming $E_{bond} = 494.4$ kJ mol^{-1}, the O-H binding energy of water. Similarly, the number of broken chemical bonds B are obtained multiplying $< D_z >$ by the same factor. For convenience, values of $\dot{B}_z$ are reported as functions of r and t in **Table 8**. From the

column $\left(\dot{B}_z\right)_{t=0}$ in **Table 1** we see that the rate of bond breaking per cell range from $\sim 10^3$ to $\sim 10^5$ d^{-1} for particles sized from 0.4 to 2.0 μm. It is worth stressing that it is immaterial whether the emitted α particles directly damage chemical bonds of biological significance or deliver their energy to water with formation of hydroxyl radicals $HO^{\cdot}$ and $H_2O^{\cdot+}$ radical cations because these reactive species are able to rapidly diffuse to the regions of the cell containing the genetic material.

CONCLUSION

The limited range in tissue of alpha particles emitted by ^{238}U considerably reduces the actual mass subjected to irradiation by ceramic particles of $^{238}U_3O_8$. Once this effect is taken into account in evaluating both the dose rate and the cumulative dose delivered to the affected tissues, 20 years after the exposure the averaged dose for $0.4 \leq r_0 \leq 2.0$ μm ranges from 6.8 mGy to 0.85 Gy for the lungs and from 8.1 mGy to 1.01 Gy for the lymph nodes. However, the body mass affected by the radiation is only a fraction of a gram and rapidly decreases with the third power of particle size.

ACKNOWLEDGEMENT

The author wishes to thank an anonymous reviewer for the significant contribution toward making this a better paper.

Figure 1. Fraction of the initial mass of U_3O_8 distributing into the two compartments following intake versus time.

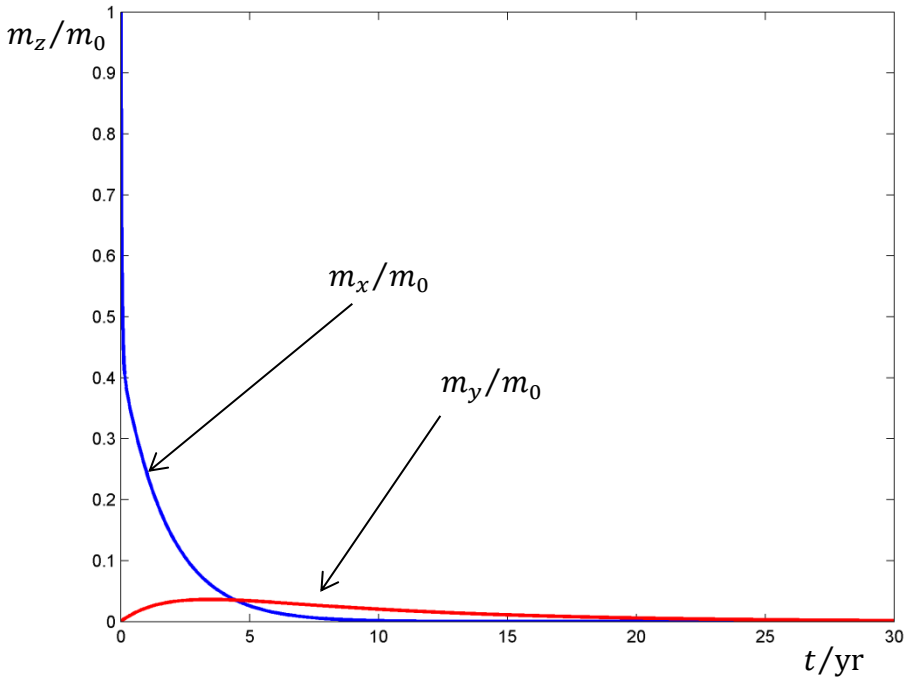

Figure 2. Fraction of the number of particles N_z/N_0 in the two compartments versus time.

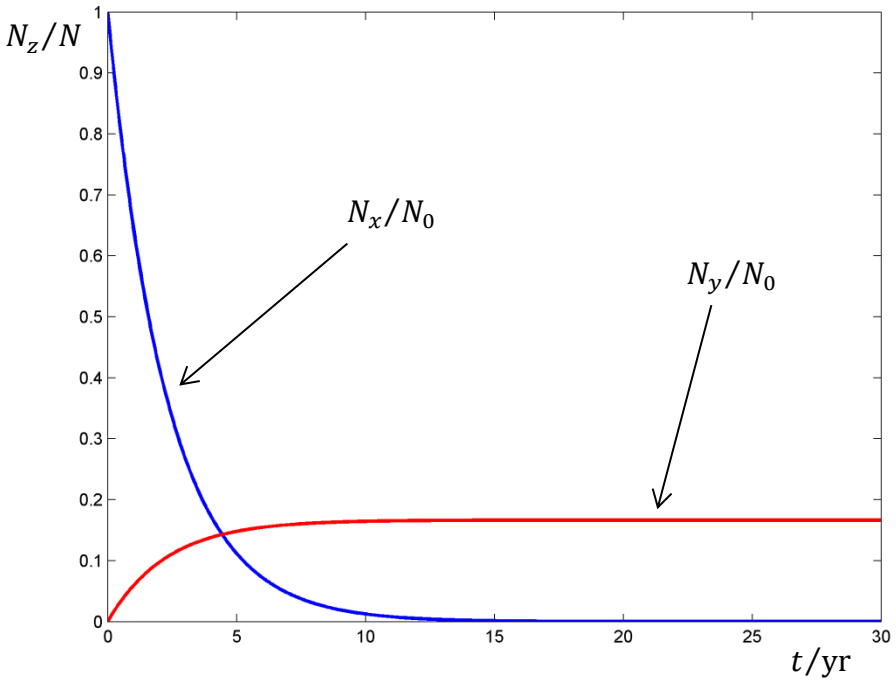

Figure 3. Plot of the dose rate $\psi_z/\mathrm{Gy\ d^{-1}}$ delivered by U_3O_8 particles with $r_0 = 1$ μm to the two compartments ($z = x, y$) versus time.

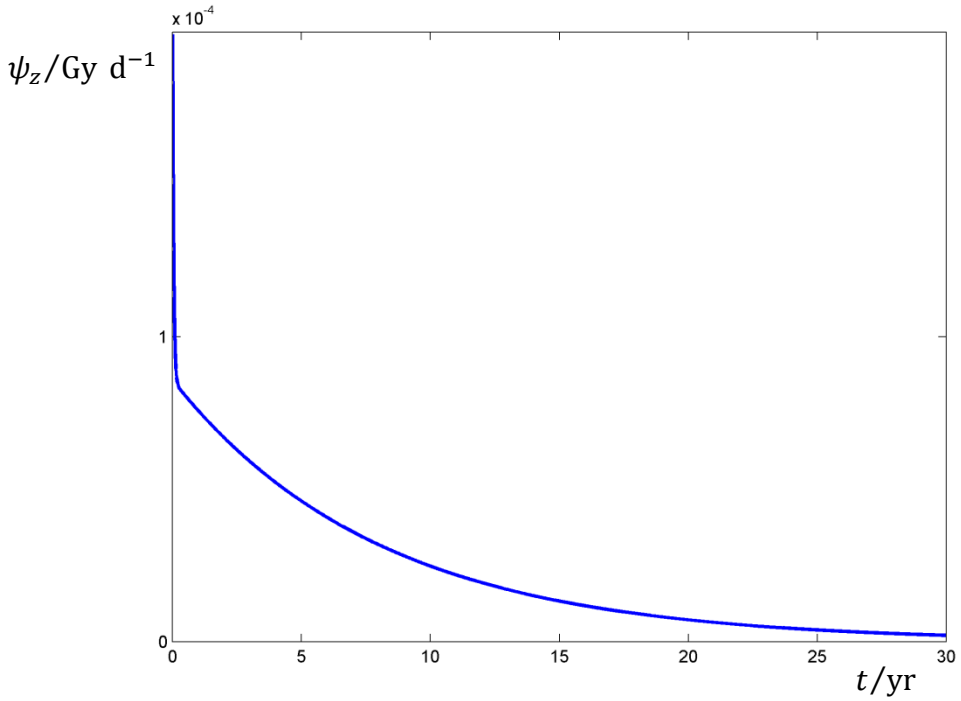

Figure 4. Plot of the dose D_z/Gy and the averaged dose $< D_z >/\mathrm{Gy}$ delivered by U_3O_8 particles with $r_0 = 1$ μm to the two compartments ($z = x, y$) versus time.

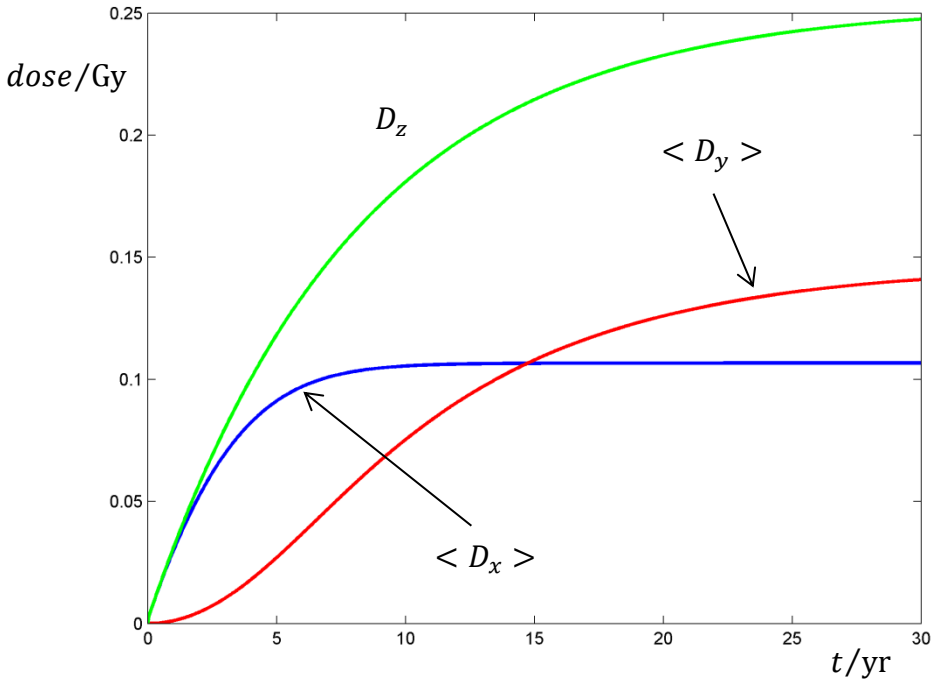

Table 1. Initial number of particles N_0 of radius r_0 in 15.51 μg of U_3O_8, the estimated number of affected cells, the initial dose rate, and the initial rate of bond breaking.

$r_0/\mu m$	N_0	cells	$\psi_0/\mathrm{Gy\ d^{-1}}$	$\left(\dot{B}_z\right)_{t=0}/\mathrm{d^{-1}}$
0.4	6.95E+06	1.08E+07	1.28E-05	1.09E+03
0.6	2.06E+06	3.20E+06	4.30E-05	3.68E+03
0.8	8.68E+05	1.35E+06	1.02E-04	8.72E+03
1.0	4.45E+05	6.92E+05	1.99E-04	1.70E+04
1.2	2.57E+05	4.01E+05	3.44E-04	2.94E+04
1.4	1.62E+05	2.52E+05	5.47E-04	4.67E+04
1.6	1.09E+05	1.69E+05	8.16E-04	6.97E+04
1.8	7.62E+04	1.19E+05	1.16E-03	9.93E+04
2.0	5.56E+04	8.65E+04	1.59E-03	1.36E+05

Table 2. Irradiated mass of the lungs M_x/g following intake of 15.51 μg of U_3O_8 particles of initial radius r_0 at various times after the exposure.

$r_0/\mu m$	1 yr	5 yr	10 yr	20 yr
0.4	4.88E-01	8.46E-02	9.46E-03	1.18E-04
0.6	1.45E-01	2.51E-02	2.80E-03	3.50E-05
0.8	6.11E-02	1.06E-02	1.18E-03	1.48E-05
1.0	3.13E-02	5.42E-03	6.05E-04	7.56E-06
1.2	1.81E-02	3.13E-03	3.50E-04	4.37E-06
1.4	1.14E-02	1.97E-03	2.21E-04	2.75E-06
1.6	7.63E-03	1.32E-03	1.48E-04	1.85E-06
1.8	5.36E-03	9.29E-04	1.04E-04	1.30E-06
2.0	3.91E-03	6.77E-04	7.57E-05	9.45E-07

Table 3. Irradiated mass in the lymph nodes M_y/g following intake of 15.51 μg of U_3O_8 particles of initial radius r_0 at various times after the exposure.

$r_0/\mu m$	1 yr	5 yr	10 yr	20 yr
0.4	4.48E-02	1.12E-01	1.25E-01	1.26E-01
0.6	1.33E-02	3.32E-02	3.69E-02	3.74E-02
0.8	5.60E-03	1.40E-02	1.56E-02	1.58E-02
1.0	2.87E-03	7.17E-03	7.97E-03	8.07E-03
1.2	1.66E-03	4.15E-03	4.61E-03	4.67E-03
1.4	1.04E-03	2.61E-03	2.91E-03	2.94E-03
1.6	7.00E-04	1.75E-03	1.95E-03	1.97E-03
1.8	4.91E-04	1.23E-03	1.37E-03	1.38E-03
2.0	3.58E-04	8.97E-04	9.97E-04	1.01E-03

Table 4. Dose rate ψ_z (Gy d^{-1}) delivered to a mass M of the lungs and lymph nodes upon intake of 15.51 μg of U_3O_8 particles of initial radius r_0 at various times after the exposure.

$r_0/\mu m$	1 yr	5 yr	10 yr	20 yr
0.4	4.84E-06	2.95E-06	1.58E-06	4.58E-07
0.6	1.63E-05	9.95E-06	5.35E-06	1.54E-06
0.8	3.87E-05	2.36E-05	1.27E-05	3.66E-06
1.0	7.57E-05	4.61E-05	2.48E-05	7.15E-06
1.2	1.31E-04	7.96E-05	4.28E-05	1.24E-05
1.4	2.08E-04	1.26E-04	6.79E-05	1.96E-05
1.6	3.10E-04	1.89E-04	1.01E-04	2.93E-05
1.8	4.41E-04	2.69E-04	1.44E-04	4.17E-05
2.0	6.05E-04	3.68E-04	1.98E-04	5.72E-05

Table 5. Dose D_z (Gy) absorbed by a mass M of the lungs and lymph nodes upon intake of 15.51 μg of U_3O_8 particles of initial radius r_0 at various times after the exposure.

$r_0/\mu m$	1 yr	5 yr	10 yr	20 yr
0.4	1.99E-03	7.56E-03	1.16E-02	1.49E-02
0.6	6.71E-03	2.55E-02	3.91E-02	5.02E-02
0.8	1.59E-02	6.05E-02	9.26E-02	1.19E-01
1.0	3.11E-02	1.18E-01	1.81E-01	2.33E-01
1.2	5.37E-02	2.04E-01	3.13E-01	4.02E-01
1.4	8.52E-02	3.24E-01	4.96E-01	6.38E-01
1.6	1.27E-01	4.84E-01	7.41E-01	9.53E-01
1.8	1.81E-01	6.89E-01	1.05E+00	1.36E+00
2.0	2.48E-01	9.46E-01	1.45E+00	1.86E+00

Table 6. Averaged dose $< D_x > /\mathrm{Gy}$ absorbed by a mass M_x of the lungs upon intake of 15.51 μg of U_3O_8 particles of initial radius r_0 at various times after the exposure.

$r_0/\mu m$	1 yr	5 yr	10 yr	20 yr
0.4	1.91E-03	5.83E-03	6.75E-03	6.83E-03
0.6	6.46E-03	1.97E-02	2.28E-02	2.30E-02
0.8	1.53E-02	4.67E-02	5.40E-02	5.46E-02
1.0	2.99E-02	9.12E-02	1.05E-01	1.07E-01
1.2	5.17E-02	1.58E-01	1.82E-01	1.84E-01
1.4	8.20E-02	2.50E-01	2.89E-01	2.93E-01
1.6	1.22E-01	3.73E-01	4.32E-01	4.37E-01
1.8	1.74E-01	5.32E-01	6.15E-01	6.22E-01
2.0	2.39E-01	7.29E-01	8.44E-01	8.53E-01

Table 7. Averaged dose $< D_y >$/Gy absorbed by a mass M_y of the lymph nodes upon intake of 15.51 μg of U_3O_8 particles of initial radius r_0 at various times after the exposure.

r_0/μm	1 yr	5 yr	10 yr	20 yr
0.4	7.43E-05	1.73E-03	4.82E-03	8.06E-03
0.6	2.51E-04	5.84E-03	1.63E-02	2.72E-02
0.8	5.94E-04	1.38E-02	3.86E-02	6.45E-02
1.0	1.16E-03	2.70E-02	7.54E-02	1.26E-01
1.2	2.01E-03	4.67E-02	1.30E-01	2.18E-01
1.4	3.19E-03	7.42E-02	2.07E-01	3.46E-01
1.6	4.75E-03	1.11E-01	3.09E-01	5.16E-01
1.8	6.77E-03	1.58E-01	4.40E-01	7.35E-01
2.0	9.29E-03	2.16E-01	6.03E-01	1.01E+00

Table 8. Rate of bond breaking per affected cell $\dot{B}_z/\mathrm{d}^{-1}$ in the lungs and lymph nodes caused by the radiation delivered by 15.51 μg of U_3O_8 particles of initial radius r_0 to the mass M of tissue at various times after the exposure.

r_0/μm	1 yr	5 yr	10 yr	20 yr
0.4	4.14E+02	2.52E+02	1.35E+02	3.91E+01
0.6	1.40E+03	8.50E+02	4.57E+02	1.32E+02
0.8	3.31E+03	2.01E+03	1.08E+03	3.13E+02
1.0	6.47E+03	3.93E+03	2.11E+03	6.11E+02
1.2	1.12E+04	6.80E+03	3.65E+03	1.06E+03
1.4	1.77E+04	1.08E+04	5.80E+03	1.68E+03
1.6	2.65E+04	1.61E+04	8.66E+03	2.50E+03
1.8	3.77E+04	2.29E+04	1.23E+04	3.56E+03
2.0	5.17E+04	3.15E+04	1.69E+04	4.89E+03

REFERENCES

1. Lind, O.C., Salbu, B., Skipperud, L., Janssens, K., Jaroszewicz, J. and De Nolf, W. *Solid state speciation and potential bioavailability of depleted uranium particles from Kosovo and Kuwait.* Journal of Environmental Radioactivity **100**, 301–307 (2009).
2. Miller, A.C., Bonait-Pellie, C., Merlot, R.F., Michel, J., Stewart, M. and Lison, P.D. *Leukemic transformation of hematopoietic cells in mice internally exposed to depleted uranium.* Molecular and Cellular Biochemistry **279**, 97–104 (2005).
3. Miller, A.C. and McClain, D. *A Review of Depleted Uranium Biological Effects: In Vitro and In Vivo Studies.* Reviews on Environmental Health **22**, 75–89 (2007).
4. Bland, D., Rona, R., Coggon, D., Anderson, J., Greenberg, N., Hull, L. and Wessely, S. *Urinary isotopic analysis in the UK Armed Forces: no evidence of depleted uranium absorption in combat and other personnel in Iraq.* Occupational and Environmental Medicine **64**, 834–838 (2007).
5. Busby, C., Hamdan, M. and Ariabi, E. *Cancer, Infant Mortality and Birth Sex-Ratio in Fallujah, Iraq 2005–2009.* Int. J. Environ. Res. Public Health **7**, 2828-2837 (2010).
6. Bleise, A., Danesi, P.R. and Burkart, W. *Properties, use and health effects of depleted uranium (DU): a general overview.* Journal of Environmental Radioactivity **64**, 93–112 (2003).
7. Chazel, V., Gerasimo, P., Dabouis, V., Laroche, P. and Paquet, F. *Characterisation and dissolution of depleted uranium aerosols produced during impacts of kinetic energy penetrators against a tank.* Radiation Protection Dosimetry **105**, 163–166 (2003).
8. Durante, M. and Pugliese, M. *Depleted uranium residual radiological risk assessment for Kosovo sites.* Journal of Environmental Radioactivity **64**, 237–245 (2003).
9. Uijt de Haag, P.A.M., Smetsers, R.C.G.M., Witlox, H.W.M., Krüs, H.W. and Eisenga, A.H.M. *Evaluating the risk from depleted uranium after the Boeing 747-258F crash in Amsterdam, 1992.* Journal of Hazardous Materials **A76**, 39–58 (2000).
10. Valdés, M. *Estimating the lung burden from exposure to aerosols of depleted uranium.* Radiation Protection Dosimetry **134**, 23–29 (2009).
11. Bem, H. and Bou-Rabee, F. *Environmental and health consequences of depleted uranium use in the 1991 Gulf War.* Environment International **30**, 123–134 (2004).
12. ASTAR (NIST, National Institute of Standards and Technology): *Stopping power and range tables for helium ions:* http://physics.nist.gov/PhysRefData/Star/Text/ASTAR.html.
13. Poncy, J-L., Metivier, H., Dhilly, M., Verry, M. and Masse, R. *In vitro dissolution of uranium oxide by baboon alveolar macrophages.* Environmental Health Perspectives **97**, 127-130 (1992).
14. Wrenn, M.E., Bertelli, L., Durbin, P.W., Singh, N.P., Lipsztein, J.L. and Eckerman, K.F. *A Comprehensive Metabolic Model for Uranium Metabolism and Dosimetry Based on Human and Animal Data.* Radiation Protection Dosimetry **53**(1-4), 255-258 (1994).
15. Miller, A.C., Stewart, M., Brooks, K., Shi, L. and Page, N. *Depleted uranium-catalyzed oxidative DNA damage: absence of significant alpha particle decay.* Journal of Inorganic Biochemistry **91**, 246–252 (2002).